Remote sensing investigation of inundation, elevation and land use assessment in Moscow state, Russia

K. Choudhary[1], M.S. Boori[1,2], A. Kupriyanov[1, 3]

[1]Samara National Research University, Moskovskoye Shosse 34A, Samara, Russia, 443086
[2]American Sentinel University, 2260 South Xanadu Way, Suite 310, Aurora, Colorado, USA
[3]Image Processing Systems Institute of RAS - Branch of the FSRC "Crystallography and Photonics" RAS, Molodogvardejskaya street 151, Samara, Russia, 443001

Abstract. Land use/cover expansion is one of the major drivers of regional environmental change. With increasing scientific and political interest in regional aspects of global environmental changes, there is a strong stimulus to better understand the patterns causes and environmental consequences of LULC expansion in the elevation of Moscow state, one of the areas in the nation with fast economic growth and high population density. Satellite remote sensing images (Landsat TM, ETM and OLI) were employed to detect land cover changes. A 70 to 300 m inundation land loss scenarios for surface water and sea level rise (SLR) were developed using digital elevation models of study site topography through remote sensing and GIS techniques by ASTER GDEM and Landsat OLI data. The most severely impacted sectors are expected to be the vegetation, wetland and the natural ecosystem. Improved understanding of the extent and response of SLR will help in preparing for adaptation.

Keywords: Remote Sensing, Inundation, Land use assessment.

1. Introduction

Russia has a largely continental climate because of its sheer size and compact configuration. Most of its land is more than 400 km. from the sea and the centre is 3,840 km. from the sea. Russia's mountain ranges, predominantly to the south and the east, block moderating temperatures from the Indian and Pacific Oceans but European Russia and northern Siberia lack such topographic protection from the Arctic and North Atlantic Oceans. Moscow located in European Russia. It's the area of high environment sensitivity zone due to harsh climate conditions with maximum time frozen temperature below then zero [1-2]. The region is drained by numerous rivers and dotted with lakes due to heavy rainfall. Numerous studies have been performed to understand the variations in the Land surface temperature as a result of changes in the land surface properties. Since the 1960s, scientists have extracted and modelled various vegetation biophysical variables using remote sensing data and the normalized difference vegetation index is one such widely adopted index. Inverse relationship has been reported between land surface temperature and vegetation index. Nowadays, it is recognize that climate change and sea level rise will impact seriously upon the natural environment and human society in the area [3-4]. There for sea level rise has to be one of the main impacts of climate change in

Moscow. Presently remote sensing and GIS techniques are the powerful tool to investigate, predict and forecast environmental change scenario in a reliable, non-invasive, rapid and cost effective way with considerable decision making strategies. The main aim of this research work is to describe natural hazards impacts and land loss due to water level inundation from 70 to 300m in Volga river basin located in Moscow [5-6].

2. Study Area

Moscow region an important historical, cultural, social and economic center in Russian Federation was selected for this study (fig.1). Moscow is the one of the most densely populated regions in the country and is the second most populated federal region. The Oblast has no official administrative canter, it is public authorities are located in Moscow and across other locations in the Oblast. As of the 2010 Census, its population was 7,095,120 and 7,23,1068 recorded in the 2015 Census. The latitude of the city is 55° 45’ 7” N and longitude is 37° 36’ 56" E. The region is highly industrialized, such as metallurgy, oil refining, mechanical engineering, food, energy and chemical industries [7-8].

The climate of Moscow region is humid continental, short but warm summers and long cold winters. The average temperature is 3.5 °C (38.3 °F) to 5.5 °C (41.9 °F). The coldest months are January and February average temperature of −9 °C (16 °F) in the west and −12 °C (10 °F) in the east. The minimum temperature is −54 °C (−65 °F). Here are more than three hundred rivers in Moscow regions and most rivers belong to the basin of the Volga [9]. Which itself only crosses a small part in the north of Moscow region. They are mostly fed by melting snow and the flood fall on April-May. The water level is low in summer and increases only with heavy rain [10-11]. The river freezes over from late November until April.

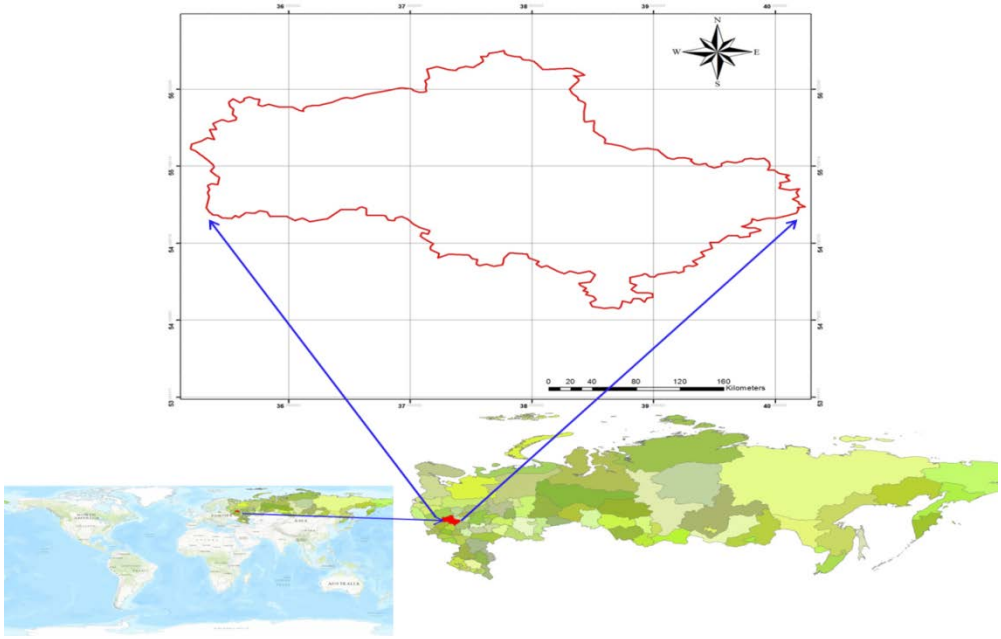

Figure 1. Location map of the study area in Moscow Region, Russia.

3. Data and Methodology

3.1 Data

In this research work we used primary (satellite data) and secondary data such as ground truth for land use/cover classes and topographic sheets. The ground truth data were collected using Global Positioning System (GPS) for the year of 2015 in the month of June to August for image analysis and classification accuracy [12-13]. The specific satellite images used were Landsat OLI (Operational Land Imager) for landscape and Advanced Space borne Thermal Emission and Reflection Radiometer (ASTER) Global Digital Elevation Model (ASTER GDEM) for elevation information.

3.2 *Image pre-processing and classification*

In pre-processing, first all images were georeferenced by WGS 1984 UTM projection, later on calibrated and remove there errors/dropouts. We use specific band combination and use image enhancement techniques such as histogram equalization to improve the classification accuracy[14]. At this stage, 50 points were selected as GCPs (Ground Control Points) for all images. Data sources used for the GCP selection were: digital topographic maps, GPS (Global Positioning Points) acquisitions. The data of ground truth were adapted for each single classifier produced by its spectral signatures for producing classification maps. For land use/cover classification, supervised maximum likelihood algorithm (MLC) was used in ArcGIS 10.2 software. MLC classification is based on training sites (signature) provided by the analyser based on his experience [15-16]. After training site whole image classified according to similar digital value of training site and finally classification give land use classified image of the area (fig.2). Seven main land use/cover classes have been find namely agriculture, barren land, forest, settlements, scrubland, water body and wetland in the study area (table. 1).

Table 1. Classes delineated on the basis of supervised classification.

Class name	Description
Agricultural	Cultivated areas, crop lands, grass lands, vegetables, fruits etc.
Barren land	This contains open lands mostly barren but also small vegetation.
Forest	Small trees and shrub vegetation area except for vegetation.
Scrubland	Scrub is a plant community describe by vegetation shrubs, often also including grasses and herbs.
Settlements	Includes construction activities along the coastal dunes as well as sporadic houses within the local village and some governmental buildings.
Water body	All the water within land mainly river, ponds, lakes etc.
Wetland	A wetland is a land area with standing water and low soil fertility.

A preparative requirement for the analysis of flooding impacts was the development of spatial datasets. A 1m spatial resolution digital elevation model (DEM) with error within 224 mm in elevation was constructed using ASTER GDEM images (fig.2). The GIS environment was used to classify and map the topology of land threatened by inundation [17].

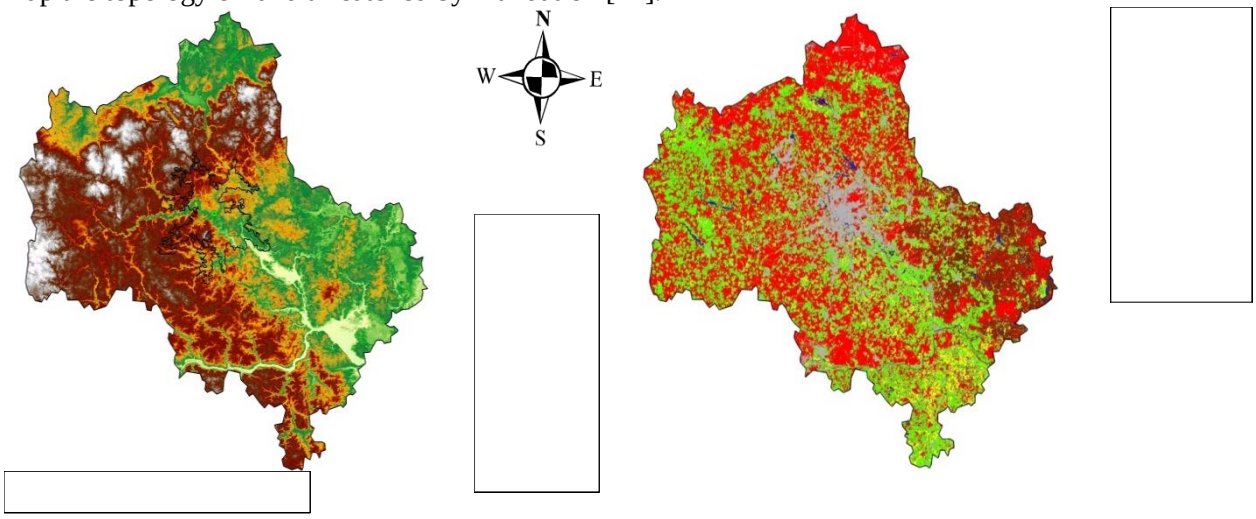

Figure 2. Elevation and land use/cover map of Moscow, Russia.

The length of the sand spit at some places is more than 1km and they are highly vulnerable to river erosion basin.

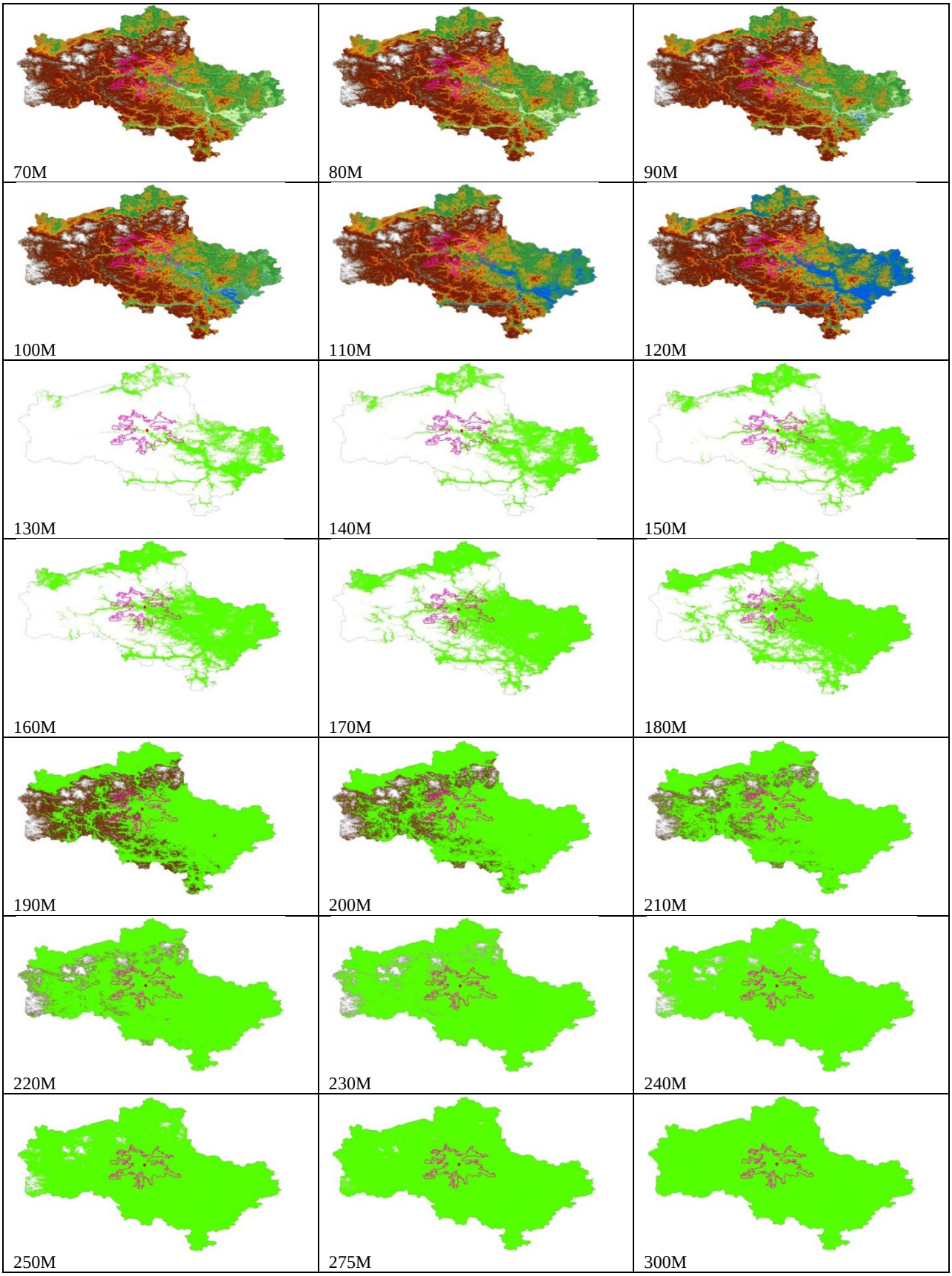

Figure 3. Land areas vulnerable to inundation in the Moscow, Russia.

4. Results

The DEM presented in figure 3 shows that low-lying land is more extensive at the north and canter of the study area. The areas lower than 1m above mean sea level (MSL), which are at risk of inundation under the minimum inundation level are vegetation, industry and urban area basically whole city.

5. Land loss due to inundation

The main results of land loss due to inundation are presented in Figure 4. The most significant changes would occur south-east side of the Moscow.

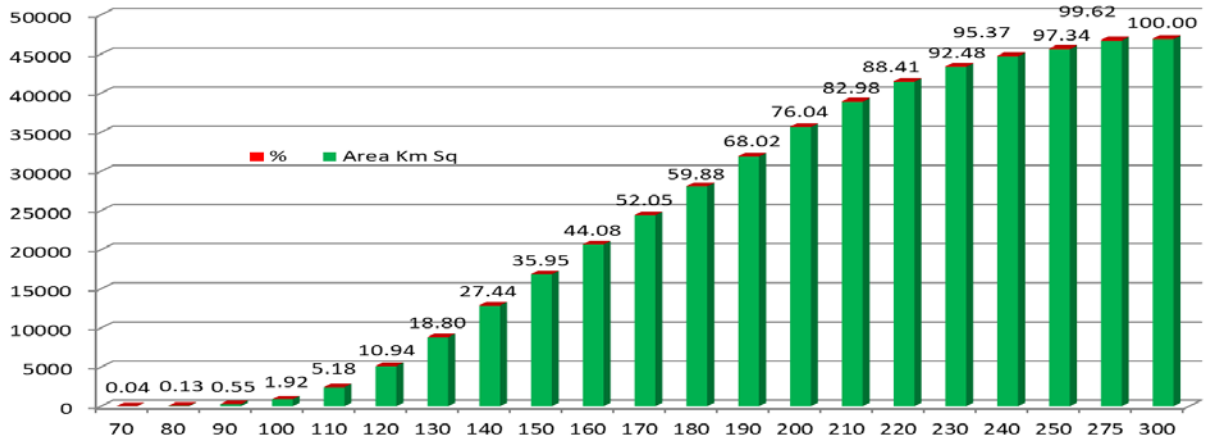

Figure 4. Inundation area graph of the Moscow, Russia.

At the minimum inundation level (70m in fig.4), 0.04% (20.24 km^2) of the total area (table 2) would be flooded including: urban areas, natural vegetation and agricultural land and beaches.

The area of submergence for 80m rise in water level is up to 60.12 km^2 (0.13%) and subsequently for 90m 258.29 km^2 (0.55%), 100m 895.84 km^2 (1.92%), 110m 2417.18 km^2 (5.18%), 120m 5108.59 km^2 (10.94%), 130m 8779.34 km^2 (18.80), 140m 12815.38 km^2(27.44%), 150m 16792.16 km^2 (35.95%), 180m 27976.67 km^2 (59.88%), 210m 38787.89 km^2 (82.98%), 240m 44584.13 km^2 (95.37%), 275m 46578.68 km^2 (99.62%) and 300m 46754.70 km^2 (100%) respectively (table 2). From the land use/cover map, it is clear that the maximum area is covered by agriculture which include Moscow city. At the full inundation level 300m in fig. Such a loss of land implies that the population living presently in these areas would be displaced. Even if some parts of the ecosystem of the wetland are not destroyed, because those parts could adapt to sea level rise and move landwards, the species richness is likely to decrease, due to repugnant new conditions where several plant communities and rare species would disappear. The area least vulnerable to inundation would be the southern and east part of the study area. However, parts of city and port, as well as an important river beach and natural forest would be flooded.

6. Conclusion

Based on multi-temporal Landsat images, we determined that there was significant expansion of anthropogenic land cover in the Moscow. Analysis revealed that the area of anthropogenic land cover was increased, resulting in a substantial reduction in natural land cover. The inundation maps can be overlaid on land use/cover maps to find out the extent of submergence of different land use/cover areas [18]. By contrast, arable land declined by 10% due to occupation by urbanization and industrialization. It is necessary to incorporate the elevation levels for new settlements areas under the town planning acts so that human life and property are saved from natural hazards. The run-up levels can be used as guidance to determine safe locations of settlements from river basin.

Table 2. Potential land loss of the main sectors for 70m to 300m inundation levels scenarios (in km2 and in % of the total inundated areas).

	70M		80M		90M		100M		110M		120M		130M	
Class name	km²	%	km²	%	km²	%	km²	%	km²	%	km²	%	km²	%
Agriculture	4.92	24.32	22.86	38.02	119.46	46.25	388.84	43.41	853.78	35.32	1581.83	30.96	2557.14	29.13
Barren land	2.35	11.62	6.56	10.91	27.79	10.76	99.96	11.16	285.46	11.81	564.95	11.06	866.86	9.87
Forest	3.38	16.68	9.33	15.52	37.41	14.48	123.66	13.80	364.95	15.10	1001.52	19.60	2184.16	24.88
Scrubland	6.18	30.54	12.33	20.51	39.49	15.29	157.59	17.59	549.33	22.73	1182.53	23.15	1812.09	20.64
Settlements	1.66	8.18	4.23	7.04	16.80	6.50	71.10	7.94	229.20	9.48	542.06	10.61	1031.46	11.75
Water body	1.30	6.41	3.69	6.14	12.58	4.87	36.90	4.12	90.60	3.75	143.23	2.80	186.29	2.12
Wetland	0.45	2.24	1.12	1.86	4.76	1.84	17.79	1.99	43.85	1.81	92.48	1.81	141.34	1.61
Total	20.24	0.04	60.12	0.13	258.29	0.55	895.84	1.92	2417.18	5.18	5108.59	10.94	8779.34	18.80
	140M		150M		160M		170M		180M		190M		200M	
Class name	km²	%	km²	%	km²	%	km²	%	km²	%	km²	%	km²	%
Agriculture	3605.91	28.14	4651.49	27.70	5722.11	27.79	6903.08	28.39	8202.99	29.32	9545.05	30.03	10772.92	30.31
Barren land	1159.12	9.04	1448.88	8.63	1724.89	8.38	2000.08	8.23	2266.48	8.10	2506.25	7.88	2689.91	7.57
Forest	3667.29	28.62	5188.49	30.90	6621.71	32.16	7975.34	32.80	9352.34	33.43	10959.28	34.48	12840.17	36.13
Scrubland	2363.85	18.45	2793.90	16.64	3072.01	14.92	3225.66	13.27	3291.92	11.77	3317.75	10.44	3332.07	9.38
Settlements	1627.70	12.70	2272.80	13.53	2939.31	14.27	3611.60	14.85	4225.56	15.10	4780.97	15.04	5198.22	14.63
Water body	219.43	1.71	240.84	1.43	299.20	1.45	370.93	1.53	394.77	1.41	418.45	1.32	431.27	1.21
Wetland	172.08	1.34	195.77	1.17	213.47	1.04	227.91	0.94	242.61	0.87	258.15	0.81	273.61	0.77
Total	12815.38	27.44	16792.16	35.95	20592.70	44.08	24314.60	52.05	27976.67	59.88	31785.89	68.02	35538.18	76.04
	210M		220M		230M		240M		250M		275M		300M	
Class name	km²	%	km²	%	km²	%	km²	%	km²	%	km²	%	km²	%
Agriculture	11770.03	30.34	12506.84	30.26	13040.38	30.16	13413.83	30.09	13655.11	30.01	13881.56	29.80	13902.42	29.73
Barren land	2813.50	7.25	2886.41	6.98	2933.22	6.78	2962.56	6.64	2980.15	6.55	2992.10	6.42	2992.95	6.40
Forest	14680.51	37.85	16235.11	39.28	17450.69	40.37	18331.89	41.12	18951.63	41.64	19740.06	42.38	19889.92	42.54
Scrubland	3342.19	8.62	3350.29	8.11	3357.22	7.77	3362.99	7.54	3368.20	7.40	3376.74	7.25	3377.19	7.22
Settlements	5459.78	14.08	5620.17	13.60	5716.00	13.22	5776.87	12.96	5815.11	12.78	5847.92	12.55	5851.71	12.52
Water body	437.79	1.13	441.77	1.07	444.10	1.03	445.60	1.00	446.68	0.98	449.23	0.96	449.42	0.96
Wetland	284.08	0.73	287.53	0.70	289.38	0.67	290.39	0.65	290.77	0.64	291.07	0.62	291.09	0.62
Total	38787.89	82.98	41328.12	88.41	43230.99	92.48	44584.13	95.37	45507.66	97.34	46578.68	99.62	46754.70	100.00

7. Acknowledgements

This work was supported by the Federal Agency of Scientific Organizations (agreement No 007-ГЗ/Ч3363/26) and the Ministry of education and science of the Russian Federation; by the Russian Foundation for Basic Research grants (# 16-41-630761; # 16-29-11698, # 17-01-00972).

8. References

[1] Tabak, N.M. Simulating the Effects of Sea Level Rise on the Resilience and Migration of Tidal Wetlands along the Hudson River / N.M. Tabak, M. Laba, S. Spector // PLoS ONE. – 2016. – Vol. 11(4). – P. 0152437. DOI: 10.1371/journal.pone.

[2] Boori, M.S. Global Land Cover classification based on microwave polarization and gradient ratio (MPGR) / M.S. Boori, R.R. Ferraro // Geo-informatics for Intelligent Transportation, Springer International Publishing Switzerland. – 2015. – Vol. 71. – P. 17-37. DOI: 10.1007/978-3-319-11463-7-2.

[3] Yang, Z. Estuarine response to river flow and sea-level rise under future climate change and human development / Z. Yang, T. Wang, N. Voisin, A. Copping // Estuarine, Coastal and Shelf Science. – 2015. – Vol. 156. – P. 19-30.

[4] McGranahan, G. The rising tide: assessing the risks of climate change and human settlements in low elevation coastal zones / G. McGranahan, D. Balk, B. Anderson // Environ. Urban. – 2017. – Vol. 19(1). – P. 17-37.

[5] Sun, X. Integrative assessment and management implications on ecosystem services loss of coastal wetlands due to reclamation / X. Sun, Y. Li, X. Zhu // J. Clean. Prod. – 2015.

[6] Cui, L. Vulnerability assessment of the coastal wetlands in the Yangtze Estuary, China to sea-level rise / L. Cui, Z. Ge, L. Yuan, L. Zhang // Estuarine, Coastal and Shelf Science. – 2015. – Vol. 156. – P. 42-51.

[7] Sweet, W.V. From the extreme to the mean: Acceleration and tipping points of coastalinundation from sea level rise / W.V. Sweet, J. Park // Earth`s future. – 2014. – Vol. 2(12). – P. 579-600.

[8] Yabuki, H. Baseline Meteorological Data in Siberia (BMDS) Version 5.0, RIGC, JAMSTEC, Yokosuka, Japan / H. Yabuki, H. Park, H. Kawamoto, R. Suzuki, V.N. Razuvaev, O.N. Bulygina, T. Ohata // Distributed by CrDAP, Digital Media, 2011.

[9] Rotzoll, K. Assessment of groundwater inundation as a consequence of sea level Rise / K. Rotzoll, C.H. Fletcher / /Nature Climate Change. – 2013. – Vol. 3. – P. 477-481.

[10] Shalaby, A. Remote sensing and GIS for mapping and monitoring land cover and land-use changes in the Northwestern coastal zone of Egypt / A. Shalaby, R. Tateishi // Appl. Geogr. - 2007. – Vol. 27(1). – P. 28-41.

[11] Shryock, H.S. The Methods and Materials of Demography / H.S. Shryock, J.S. Siegel, E.A. Larmon // US Bureau of the Census, 1973.

[12] Tian, G. Comparing urbanization patterns in Guangzhou of China and Phoenix of the USA: the Influences of Roads and Rivers / G. Tian, J. Wu // Ecol. Indic. – 2015. – Vol. 52. – P. 23-30.

[13] Thakur, A.K. Orthorectification of IRS-P6 LISS IV data using Landsat ETM and SRTM datasets in the Himalayas of Chamoli district, Uttarakhand / A.K. Thakur, S. Sing, P.S. Roy // Curr. Sci. – 2008. – Vol. 95. – P. 1459.

[14] Thomlinson, J.R. Coordinating methodologies for scaling land cover classifications from site-specific to global: steps toward validating global map products / J.R. Thomlinson, P.V. Bolstad, W.B. Cohen // Remote Sens. Environ. – 1999. – Vol. 70(1). – P. 16-28.

[15] Weng, Q. A remote sensing-GIS evaluation of urban expansion and its impact on surface temperature in the Zhujiang Delta, China / Q. Weng // Int. J. Remote Sens. – 2001. – Vol. 22. – P. 1999-2014.

[16] Courchamp, F. Climate change, sea-level rise, and conservation: keeping island biodiversity afloat / F. Courchamp, B.D. Hoffmann, J.C. Russell, C. Leclerc, C. Bellard // Trends in Ecology & Evolution. – 2014. – Vol. 29(3). – P.127-130.

[17] Boori, M.S. Four decades urban growth and land use change in Samara Russia through remote sensing and GIS techniques / M.S. Boori, K. Choudhary, A. Kupriyanov, V. Kovelskiy // SPIE Remote Sensingand Image Formation. – 2015. – Vol. 9817. – P. 01-07. DOI:10.1117/12.2227992.

[18] Rotzoll, K. Assessment of groundwater inundation as a consequence of sea-level Rise / K. Rotzoll, C.H. Fletcher // Nature Climate Change. – 2013. – Vol. 3. – P. 477-481.